scientific reports

Check for updates

OPEN

Evaluating fungal pathogen resistance across the leaf economics spectrum using the generalist fungus *Sclerotinia sclerotiorum*

Keisuke O. Watanabe[1], Kaori Kohzuma[1,3], Hiroko Kurokawa[2,3] & Kouki Hikosaka[1]✉

Leaf traits vary widely among plant species, correlating with leaf economics and growth-defense trade-offs. However, the relationship between trait variation and pathogen resistance remains unexplored. Here, we introduce a novel experimental approach to quantitatively assess pathogen resistance using the generalist fungus *Sclerotinia sclerotiorum*. In this system, leaf discs were infected either through the epidermis, evaluating physical and chemical defense, or a cut surface, solely evaluating chemical defense. We investigated pathogen resistance across 24 species ranging from annual herbs to evergreen tree species. Epidermal infection revealed higher pathogen resistance in evergreens compared with annual herb species, strongly correlated with the leaf economics spectrum. The cell wall content per leaf area explaind 61% of the interspecific variations in the pathogen resistance through epidermal infection. Pathogen resistance following cut-surface infection was associated with the accumulation of defensive chemicals, such as tannins and lignins. Our findings demonstrate how investments in physical and chemical defense enhance pathogen resistance, potentially driving evolutionarily shifts in leaf traits.

Keywords Defense, Leaf economics spectrum, Leaf functional traits, Pathogen infection, Pathogen resistance

Global leaf functional traits converge along an axis from resource-acquisitive to resource-conservative strategies across plant species, termed the leaf economics spectrum (LES)[1–4]. At one end of the axis, species exhibit higher photosynthetic rate and nitrogen concentration per unit leaf mass, lower leaf mass per area (LMA), and shorter leaf lifespan, and vice versa at the other end. This convergence arises because plants cannot simultaneously maximize photosynthetic productivity and resource conservation. A conservative strategy demands greater leaf mechanical toughness, achieved through increased investment in cell walls[5], albeit at the expense of photosynthetic capacity due to nitrogen allocation trade-offs between cell walls and photosynthetic proteins and lower CO_2 diffusivity in thicker cell walls[6–8].

What do long lifespan leaves protect against? The ecological significance of leaf mechanical toughness has been discussed primarily in terms of antiherbivory defense based on the growth-defense trade-off hypothesis[9]. Many studies have indicated that species with higher LMA experience lower herbivory rates[10–13]. However, there are many potential biotic and abiotic factors other than herbivores that physically attack leaves. The relationship between these factors and the defensive ability of leaves is not necessarily clear. This is essential for understanding what selective pressures leaf traits evolve under and what species are selected by environmental filtering.

Pathogen infection, a critical event affecting plant fitness, often through reduction of photosynthetic activity and acceleration of leaf senescence, also underscores the ecological importance of leaf mechanical toughness. Several studies have highlighted the relationship between pathogen resistance and the LES. Cronin et al.[14] observed that resource-acquisitive species (termed quick-return species in their study) were less resistant to an aphid-transmitted virus infection among grass species. Capperi et al.[15] found lower infection rates in species with higher LMA in a grassland community. Yan et al.[16] suggested that resource-acquisitive species (termed

[1]Graduate School of Life Sciences, Tohoku University, Aoba, Sendai, Japan. [2]Forestry and Forest Products Research Institute, Tsukuba, Japan. [3]Graduate School of Agriculture, Kyoto University, Kyoto, Japan. ✉email: hikosaka@tohoku.ac.jp

fast-growing species in their study) are more susceptible to fungal pathogen infection in a grassland community. However, these studies focused solely on herbaceous species. As most herbs tend toward resource-acquisitive strategies, it remains unclear whether the LES correlates with pathogen resistance across a broader LES range. Furthermore, field infection rates are influenced by factors such as host plant density and community diversity[16], which are not necessarily related with leaf traits. Although Cronin et al.[15] developed a useful experimental system to evaluate pathogen resistance, pathogen resistance in their setup may be confounded by factors such as aphid preference.

Pathogen infection rate may be limited by factors like the encounter between pathogens and host plants, pathogen growth resources, and plant tissue-level resistance. As plant functional traits are likely related only to tissue-level resistance, we require an experimental system to rule out other factors'influence. In addition, since infection by many pathogen organisms is host-specific, such organisms are not suitable to evaluate interspecific variations in pathogen resistance. To overcome these difficulties, we developed a new experimental system to assess pathogen resistance, wherein a leaf disc is infected by *Sclerotinia sclerotiorum* (Libert) de Bary. This fungus is widespread in temperate, tropic, and arid regions[17], exhibiting a broad host range and low host specificity, with over 400 species, including both herbaceous and tree species, having been documented *S. sclerotiorum* hosts[18,19] Therefore, *S. sclerotiorum* can be used to evaluate pathogen resistance across diverse plant species. To eliminate influence of factors other than leaf traits, we used *S. sclerotiorum* growing in agar plug, which contained resources for growth of the fungus, where growth and attack by *S. sclerotiorum* are free from resource limitation.

Many fungal pathogens, including *S. sclerotiorum*, invade and grow within leaf cells, necessitating penetration through two barriers: the epidermis, serving as a physical barrier, and plant defensive systems in cells, acting as a chemical barrier. To assess the efficacy of these barriers separately, we implemented two treatments in our experiment. In the first treatment, *S. sclerotiorum* accessed the leaf through its surface [epidermis treatment (EPT)], requiring penetration of both physical and chemical barriers. In the second treatment, *S. sclerotiorum* accessed the leaf through a cut surface [cut-surface treatment (CST)]. By bypassing the epidermis, this treatment allowed us to assess the impact of chemical defense only. We assessed pathogen resistance in 24 species ranging from annual herbs to evergreen trees along the LES. We hypothesized that the LES is strongly associated with pathogen resistance in the EPT and that resource-conservative species exhibit greater pathogen resistance. Additionally, we hypothesized that pathogen resistance in the CST exhibits a weaker association with the LES but is correlated with defensive compound concentrations. To test these hypotheses, we assessed key LES traits and concentrations of defensive compounds.

Materials and methods

Study site and species

We studied 24 species (three annual herbs, three perennial herbs, 10 deciduous woody species, and eight evergreen woody species; Table S1) grown at the Aobayama area, Sendai, Japan (38°15′N, 140°51′E, 50–150 m above sea level). Their habitats varied from forest gaps and forest edges to roadsides. In August–September 2021, intact leaves exposed to direct sunlight for several hours per day were collected from three or more individuals for each species, except for *Skimmia japonica*, from which leaves were collected from a single individual.

Infection experiments

We used an *S. sclerotiorum* strain (NBRC No. 9395) from the Biotechnology Center of the National Institute of Technology and Evaluation in Tokyo, Japan. The strain was subcultured in Potato Dextrose Agar gel (Nissui Corp., Japan) at 25℃ and then grown on the gel for 2 days for the infection experiments. We brought intact leaves of the studied species to our laboratory and punched out 2 discs (16 mm in diameter) per leaf from 12 fresh leaves per species using a cork polar (24 discs per species), with 12 discs each used for the EPT and the CPT. Infection experiment was started on the day of leaf sampling.

Infection was conducted in a 12-well cell culture plate (polystyrene; plate size: 128 × 86 × 20 mm; well diameter: 25 mL; Fig. 1). To prevent drying, 0.5 mL of deionized water was added to each well. A black plastic object (a lid for a glass bottle), measuring 17.5 mm in diameter and 10.0 mm in height, was placed in each well with a leaf disc placed on top to avoid its contact with the water. For the EPT, an agar plug (6 mm in diameter and 5 mm in height) was attached to the center of the abaxial side of the disc, which was then placed with the adaxial side up on the lid. For the CST, we cut the edge of the disc in a straight line, attached a halved agar plug to the cut surface, and placed the disc on the lid, slightly inclining the plate to maintain contact between the disc and the agar plug throughout the experiment. Agar plugs contained approximately 2.50 and 1.25 mg of glucose for the EPT and CST, respectively, suggesting that growth and attack by *S. sclerotiorum* might not be limited by resource availability. Each plate contained 12 discs for either the EPT or CST, with 3 control discs (agar plug without *S. sclerotiorum*) and 9 infection discs (agar plug containing *S. sclerotiorum*) per plate. One plate was used for each species.

After the setting the discs with the agar plug, the plate was sealed with a plastic cover and remained unopened during the experiment. Normal photographs and chlorophyll fluorescence images were taken 24, 48, 72, and 96 h after treatment onset using a commercial digital camera (AQUOS Sense 4, Sharp, Osaka) and a fluorescence imaging system (FluorCam 800MF, Photon System Instruments, Drásov, Czech), respectively. Given that quantitative evaluation from normal photographs was challenging for some evergreen species due to specular reflection, we used chlorophyll fluorescence images to evaluate the degree of pathogen infection. We defined noninfected areas (NIAs) as regions where the fluorescence yield of dark-adapted discs under saturating light was present and quantified their areas using ImageJ.

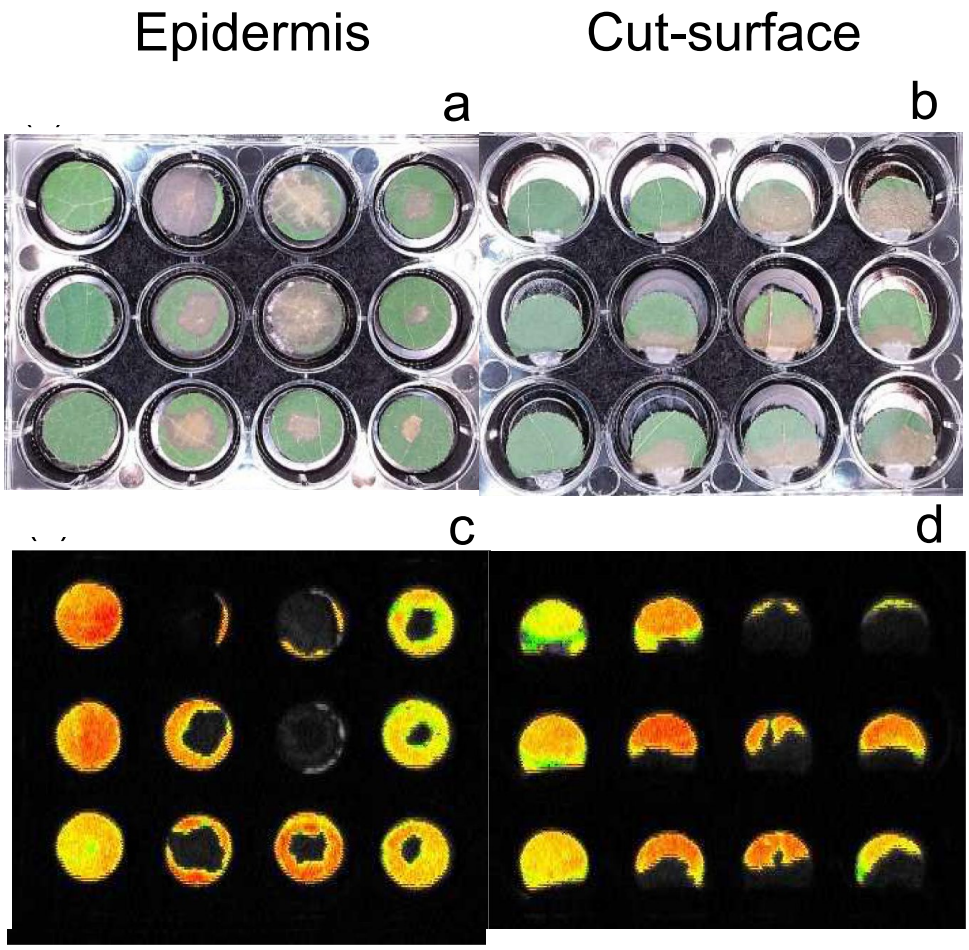

Fig. 1. Photographs (**a**, **b**) and chlorophyll fluorescence images (**c**, **d**) of treated leaf discs. **a** and **c** depict the epidermis treatment in *Mallotus japonicus*. The agar plug without *Sclerotinia sclerotiorum* (left raw; control) and with *S. sclerotiorum* (other rows) was attached to the abaxial side of the leaf disc, with the images taken from the adaxial side. **b** and **d** represent the cut-surface treatment in *Chengiopanax sciadophylloides*. The agar plug with or without *S. sclerotiorum* was attached to the cut surface, visible on the lower side of the disc in the photographs.

Trait determination

We obtained 21 discs (8 mm in diameter) from the harvested leaves of each species for trait determination. These discs were collected from 3 individuals (7 discs per individual) except for *S. japonica*. Three discs were dried in an oven at 70 °C for over 3 days, and their mass and nitrogen (N) content were measured using an elemental analyzer (UNICUBE, Elementar, Langenselbold, Germany). LMA and N concentration were calculated from these discs. The remaining 18 discs were separated into three groups (each group contain six discs) and frozen in liquid nitrogen and stored at − 85℃. From one group, Ribulose-1,5-bisphosphate carboxylase/oxygenase (Rubisco; R) content was determined following the method of Hikosaka and Shigeno[20]. From another group, soluble protein (SPR) and membrane protein (MPR) content as well as cell wall (CW) and cell wall nitrogen (NCW) content were determined using the method of Yasumura et al.[21] with modifications. The third group was used if above measurements were failed. Refer to the Supplemental Information for further details.

Parts of the remaining leaves were used for a punch test, employing a digital force gauge (DS2-50N, Imada, Aichi, Japan) to measure the maximum force required for penetration. Approximately 10 g of fresh leaves were also frozen in liquid nitrogen, stored at − 85℃, freeze-dried, and milled. The phosphorus (P), total phenol (TPH), condensed tannin (CT), and lignin (LG) content were determined following the method of Kurokawa et al.[22]. Refer to the Supplemental Information for further details.

Although we did not study important LES traits, photosynthetic rates and leaf life span, Hikosaka & Shigeno[20] showed that photosynthetic rates and leaf life span were strongly correlated with LMA across plants growing in this area.

Data analyses

Traits were expressed on both area and mass bases using the mean LMA obtained from the dried leaf discs. Mean trait values were calculated for each species ($n = 3$). Principal component analysis (PCA) was performed to assess trait variations among species. Although in LES studies, variables are generally expressed on a mass basis, we

also used area-based variables because *S. sclerotiorum* invades through leaf surface. All trait values were $\log_{10}$-transformed prior to analysis.

The relative infected area (RIA) was calculated as follows:

$$\mathrm{RIA} = 1 - \frac{\mathrm{NIA}_{\mathrm{tre}}}{\mathrm{NIA}_{\mathrm{con}}}, \tag{1}$$

where NIA is the average noninfected area of discs, with the subscripts $_{\mathrm{tre}}$ and $_{\mathrm{con}}$ denoting discs treated with *S. sclerotiorum* and lacking *S. sclerotiorum* treatment, respectively. Data from discs damaged by other factors, such as drying, were excluded. The RIA was obtained at 1, 2, 3, and 4 days after treatment.

Temporal changes in the RIA were fitted with a logistic equation (Fig. S1):

$$Y = \frac{1}{1 + \frac{1}{\exp(aX - b)}}, \tag{2}$$

where a and b are the slope and intercept of the curve, respectively. Y and X represent the RIA and the days after treatment, respectively. a represents the infection growth rate (IGR; the intial slope of the curve), whereas b determines the RIA at day 0. To obtain a reasonable value for a, we used a common value for b across species. Although the absolute value of a changes with b, the order of a among species remains constant. We used a constant value of 6.907 for b, setting the RIA at 0.001 on day 0. If the calculated value of a was negative, we applied 0 for a. Higher a values indicated lower pathogen resistance.

To assess traits determining pathogen resistance, we performed logistic regression analyses where Y was the RIA and X was the score of the first (PC1) or second (PC2) axis from the PCA traits. Using Eq. 2, both the slope (a) and intercept (b) were adjusted to obtain the best model. We also performed multivariate regression analyses with model selection, using IGR as the target variable and all studied traits as explanatory variables. All trait values were $\log_{10}$-transformed before analysis. To eliminate multicollinearity, we avoided the coexistence of variables with a variance inflation factor exceeding 10. Using all combinations and reducing variables based on the Akaike information criterion, we obtained the best model. All statistical analyses were performed using *R* v4.22.

Results

Leaf trait values exhibited considerable variation among the studied species (Fig. 2; Table S1). For N, P, and proteins, area-based variables are positioned opposite side of the mass-based variables in the PCA because the interspecific variation in LMA was greater than the mass-based variables (Fig. 2). PC1 explained 49.3% of the total trait variation as well as showing a negative correlation with N and P concentration per unit leaf mass and a positive correlation with LMA, representing the LES (Fig. 2). PC2 explained 18.8% of the total trait variation and was positively correlated with concentrations of condensed tannin, lignin, and total phenol per unit mass.

The relative infected area (RIA) increased over time following infection onset, with a tendency for faster infection rates in herbaceous species compared with woody species (Fig. S1). In the EPT, the leaf discs of herbaceous species were completely infected by day 4 of the treatment, whereas those of evergreen species maintained green portions by day 4, with three species showing no infected area. In the CST, differences among functional types were less distinct. The RIA in the EPT was significantly correlated with the PC1 score at day 2–4, whereas no significant correlations were observed between the RIA and either the PC1 or PC2 scores in the CST (Fig. 3; Table S2).

We calculated the infection growth rate (IGR), representing pathogen susceptibility, and found a significant correlation between the IGRs in the CST and EPT (Fig. 4). Most species exhibited data points near the $Y = X$ line, indicating similar pathogen susceptibility between treatments, although some species showed a higher IGR in the CST than in the EPT. Unexpectedly, certain species exhibited a lower IGR in the CST than in the EPT.

IGR in the EPT was significantly correlated with various leaf traits (Table S3), including LMA, a representative LES trait (Fig. 5a). IGR in the CST also correlated significantly with some leaf traits (Table S3). PC1 exhibited a significant correlation with both the IGRs in the EPT and CST, albeit stronger in the EPT than in the CST (Table S3), whereas PC2 was not significantly correlated with these IGRs. Applying multiple regression analysis with model selection, we identified effective traits for IGR. For the EPT, only cell wall mass per area ($\mathrm{CW}_{\mathrm{area}}$) was selected as a trait for the best model, which explained 61% of the variation (Table 1). $\mathrm{CW}_{\mathrm{area}}$ tended to be higher in evergreen species than in deciduous or herbaceous species (Fig. 5b), and IGR was significantly lower in species with higher $\mathrm{CW}_{\mathrm{area}}$ (Table 1). For the CST, condensed tannin per leaf area ($\mathrm{CT}_{\mathrm{area}}$), phosphorus per area ($\mathrm{P}_{\mathrm{area}}$), and lignin per mass ($\mathrm{LG}_{\mathrm{mass}}$) were selected in the best model (Table 1). Among these variables, only $\mathrm{CT}_{\mathrm{area}}$ significantly affected IGR, which was lower in species with higher $\mathrm{CT}_{\mathrm{area}}$ (Table 1; Fig. 5c).

Discussion

Our findings demonstrate a strong correlation between resistance to *S. sclerotiorum* infection through the epidermis and the LES, as represented by the PC1 axis. Species with higher LMA and greater leaf toughness exhibit longer leaf lifespans, partly due to enhanced resistance to pathogen infection, contributing to their overall resource conservation. Our results not only validate the trends observed in grass species[14–16] but also broaden the applicability of the LES to a wider range of species, from herbs to evergreen trees.

Among the traits examined, $\mathrm{CW}_{\mathrm{area}}$ emerged as the primary determinant of pathogen resistance in the EPT and explained 61% of the variation in IGR. *Sclerotinia sclerotiorum* penetrates the cuticle with penetration

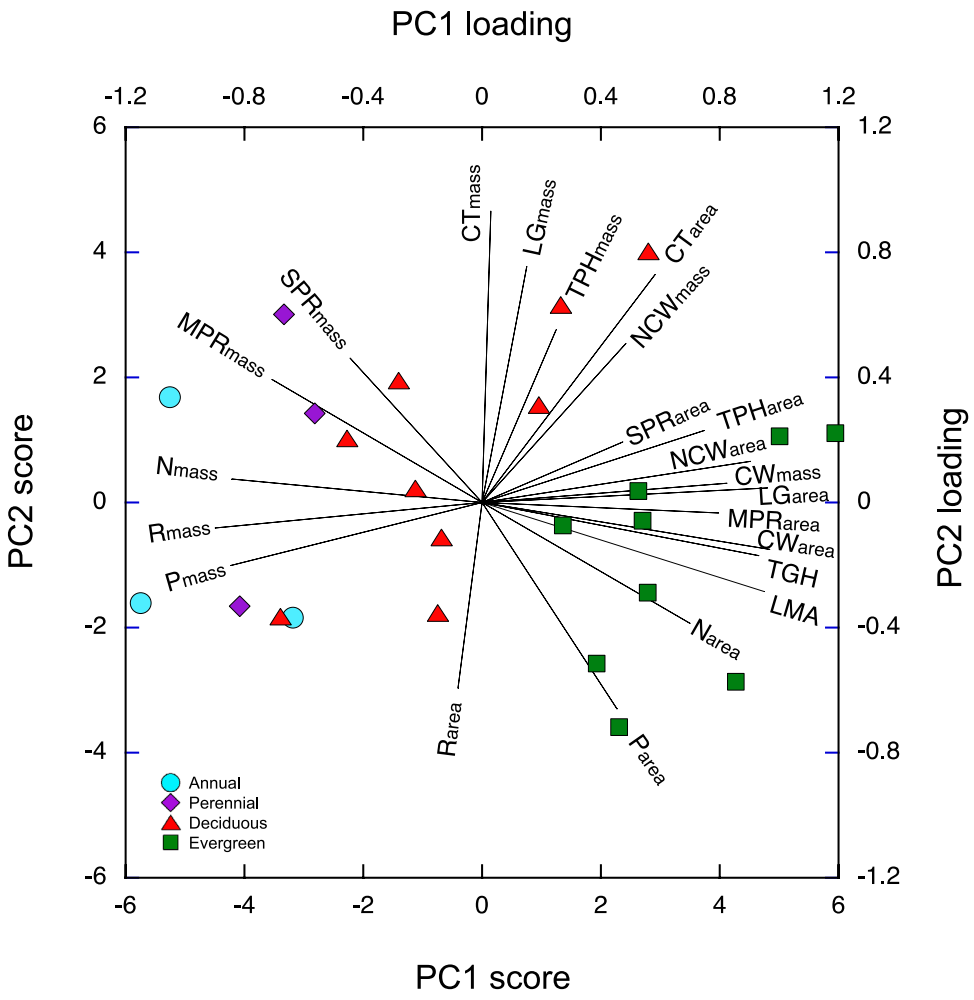

Fig. 2. Principal component analysis of the traits. Circles, diamonds, triangles, and squares denote annual herbs, perennial herbs, deciduous trees, and evergreen trees, respectively. LMA, leaf mass per area; TGH, toughness; N, nitrogen; P, phosphorus; R, Rubisco; TPH, total phenol; CT, condensed tannin; LG, lignin; SPR, soluble protein; MPR, membrane protein; CW, cell wall; NCW, cell wall nitrogen. Subscript $_{mass}$ and $_{area}$ denote leaf mass and leaf area bases, respectively.

tags, subsequently spreading subcuticularly using toxins, such as oxalic acid and cell wall–degrading enzymes, resulting in cell death[19,23]. Thicker cell walls may serve as a physical barrier against *S. sclerotiorum* infection.

We evaluated factors beyond the epidermis using the CST. A significant correlation in pathogen susceptibility between the EPT and CST suggested that factors other than epidermis may also contribute to greater pathogen resistance in the EPT. Furthermore, some species showed data distant from $Y = X$, indicating that epidermis resistance is not necessarily consistent with cut-surface resistance. In species showing higher infection rates in the CST than in the EPT, the epidermis may have played an key role in pathogen resistance. However, considering that injured tissues are less resistant to pathogens compared with healthy tissues[24], some species surprisingly exhibited lower infection rates in the CST than in the EPT. This may be attributed to wound-induced synthesis of defensive compounds, which can suppress infetion[25,26]. Such induced defenses could effectively protect cut surfaces from infection in certain species and may not be explained by leaf functional traits that are frequently determined in previous studies such as LMA and N contents.

The best model indicated that IGR in the CST is explained by CT_{area}, LG_{mass}, and P_{area}. Although the mechanisms underlying the positive contribution of P_{area} to pathogen resistance remain unclear, condensed tannins and lignins are recognized as defensive chemicals. Tannins bind to proteins, inhibiting digestion, whereas lignins strengthen cell walls. Our findings are consistent with previous studies showing that the accumulation of defensive chemicals enhances pathogen resistance[27,28]. However, compared with the EPT, correlations between IGR in the CST and leaf traits were weak. This variability may arise from diversity in chemical defense strategies among plant species.

Our results demonstrated that physical (cell walls) and chemical (tannins) investments in leaves are effective to improve resistance to infection by generalist pathogens. This would be adaptive for the plants growing in a habitat where encounter and attack of pathogens are more frequent. However, increased cell wall content comes at the expense of photosynthetic rates owing to N allocation trade-offs between the photosynthetic apparatus

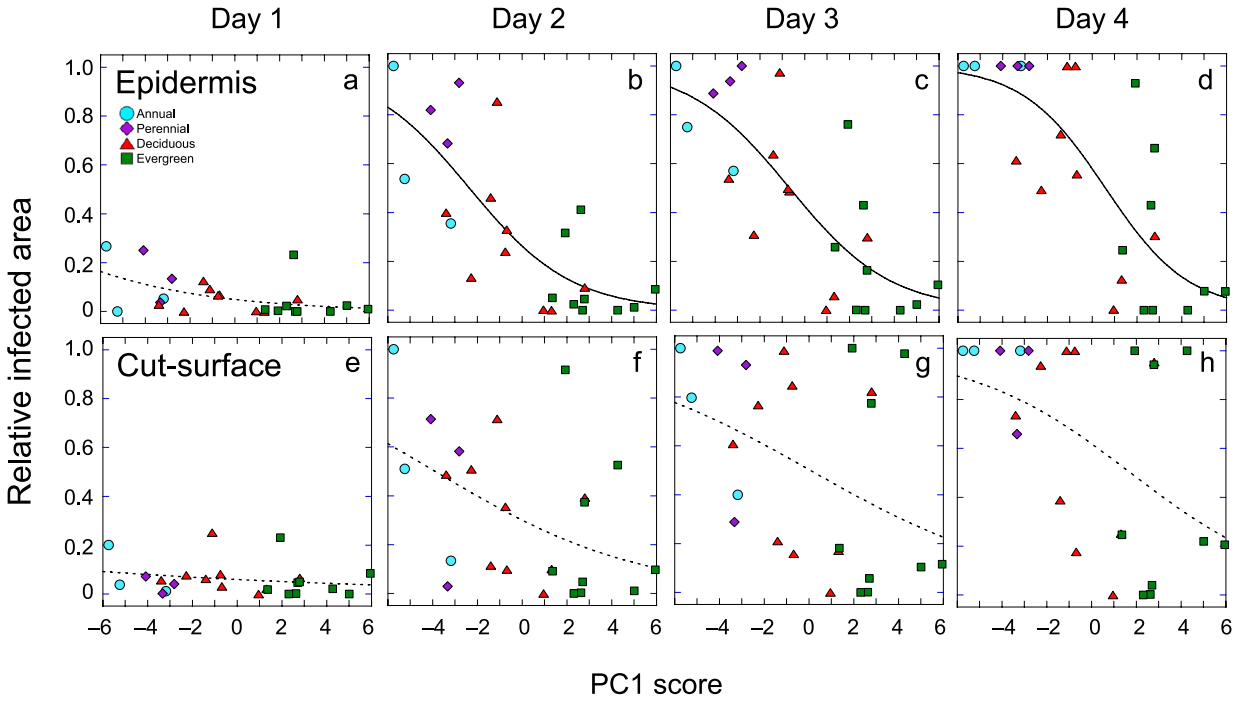

Fig. 3. Temporal change in the relative infection area as a function of the principal component score of axis 1 (PC1). Circles, diamonds, triangles, and squares denote annual herbs, perennial herbs, deciduous trees, and evergreen trees, respectively. Fitted curvilinears are a logistic equation. Continuous and dotted curves denote significant ($P < 0.05$) and nonsignificant regression coefficients, respectively. Refer to Table S2 for the regression equations.

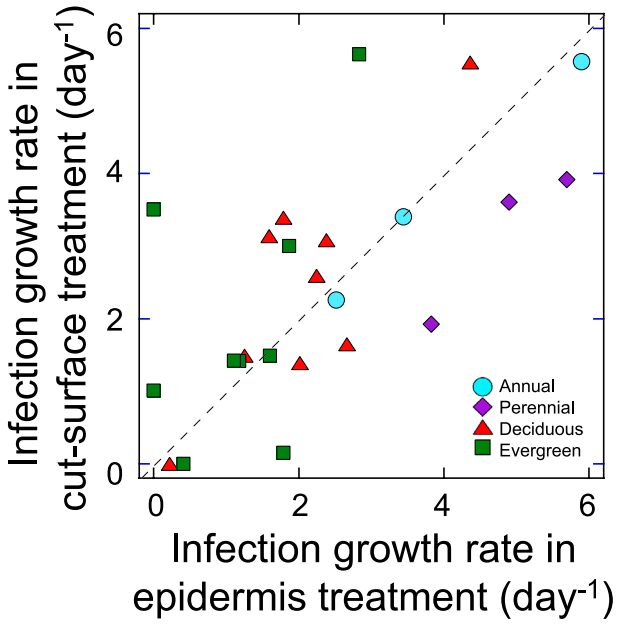

Fig. 4. Relationship of infection growth rates between the epidermis and cut-surface treatments. Circles, diamonds, triangles, and squares denote annual herbs, perennial herbs, deciduous trees, and evergreen trees, respectively. Dotted line denotes $Y = X$. Correlation between the two variables was represented by $Y = 0.99 + 0.66X$ ($R^2 = 0.45$, $P < 0.001$). Regression line is not shown in the figure.

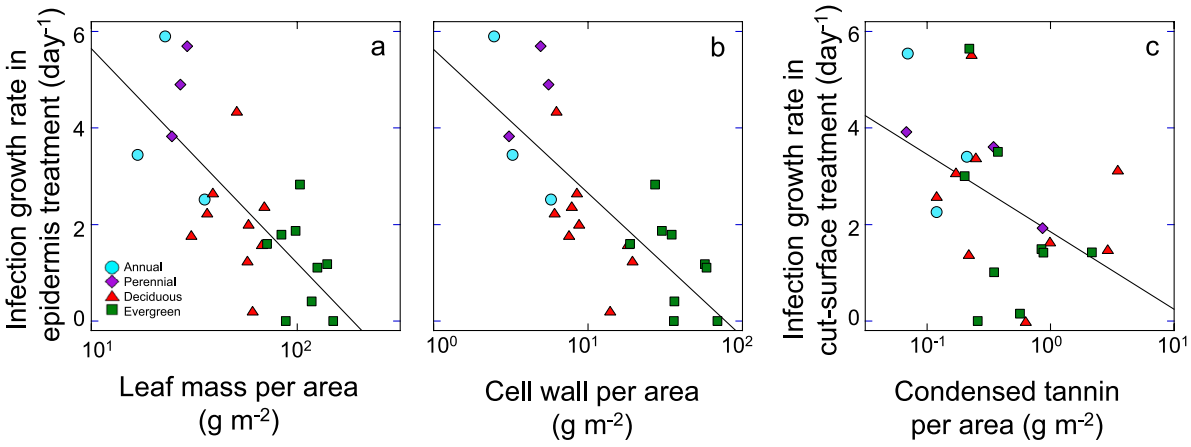

Fig. 5. Relationship between infection growth rates (IGRs) and leaf traits. (**a**, **b**) IGR in the epidermis treatment as a function of leaf mass per area (**a**) and cell wall per area (CW_{area}; **b**). (**c**) IGR in the cut-surface treatment as a function of condensed tannin per area (CT_{area}). Regression lines are $Y = 10.1 - 4.45X$ ($R^2 = 0.53$, $P < 0.001$) (**a**), $Y = 5.63 - 2.98X$ ($R^2 = 0.61$, $P < 0.001$) (**b**), and $Y = 1.85 - 1.60X$ ($R^2 = 0.21$ $P < 0.05$) (**c**), where X (trait values) is $\log_{10}$-transformed.

Epidermis treatment	Intercept	CW_{area}	R^2	AIC
	5.63 ***	−2.98 ***	0.61 ***	5.05

Cut-surface trement	Intercept	CT_{area}	P_{area}	LG_{mass}	R^2	AIC
	0.239^{NS}	−1.88 *	-3.17^{NS}	-1.92^{NS}	0.30^{+}	17.81

Table 1. The best models explaining variations in the infection growth rate. Models were selected from multiple linear regression analysis, in which all the studied traits were used as explanatory variables, based on the Akaike information criterion (AIC). Regression coefficients and their significance are shown. ***, $P < 0.001$; *, $P < 0.05$; +, $P < 0.1$; NS, $P > 0.1$. CW_{area}, cell wall mass per leaf area (g m^{-2}); CT_{area}, condensed tannin per leaf phosphorus per leaf area (g m^{-2}); P_{area}, phosphorus per leaf area (g m^{-2}); LG_{mass}, lignin per leaf mass (g g^{-1}). Trait values are log-transformed in the analysis.

and cell walls as well as the negative effects of cell wall thickness on CO_2 diffusion within mesophyll cells[6–8,29,30]. Furthermore, investments in non-photosynthetic components are oppotunity cost for photosynthesis, leading to lower growth rates of the plant[31]. If the encounter and attack of pathogens are less frequent, plants with less investments to defense are advantageous because of their higher growth rate. Therefore, there is a trade-off between growth and defense, which drives niche differentiation along LES[9].

Our results suggest that 61% of the interspecific variations in the resistance to *S. sclerotiorum* infection was explained by the variations in the cell wall amount. Other variations should be explained by factors other than LES traits. For example, thickness and chemical composition of cuticle on the epidermis might have an important role in the resistance. Interactions with phyllosphere microorganisms may also influence the resistance. Other defensive mechanisms such as production of various anti-pest proteins and compounds may also contribute to the resistance[32]. Further studies will deepen our understanding of interspecific variations in pathogen resistance. It is also needed to test whether such correlations are held in other ecosystems to generalize our conclusion.

Our new experimental system offers several advantages: 1) as *S. sclerotiorum* is a generalist fungus, we can assess pathogen resistance across a wide range of species; 2) it enables comparison of pathogen resistance among plants from different locations under standardized conditions; 3) pathogen infection rates can be quantified nondestructively; and 4) the contributions of external (epidermis) and internal (chemical defense) factors to pathogen resistance can be assessed separately. This experimental approach enhances our understanding of functional evolution in relation to pathogen resistance. However, caution is warranted when extrapolating field pathogen resistance from our results owing to differences between our experiment system and natural field conditions. Ascospores of *S. sclerotiorum* are unable to infect healthy tissues; they invade host tissues only after colonizing dead or senescent tissues saprotrophically before infecting healthy tissues[19]. This limitation may stem from resource constraints on fungal growth. In our system, the fungus can exploit ample resources contained in the agar plug, potentially leading to accelerated growth, which may not accurately reflect natural environmental conditions and the observed infection rate in our study is considered to be higher than the actual infection rate in the natural environment. However, it should be noted that the observed infection rate in our study is the rate that is free from limiting factor such as encounter of pathogen and plant and resource availability for growth and attack by pathogen. Therefore, this represents the potential rate of phathogen infection. Another caution is that infection by many pathogenic fungi on host plants is species-specific, making it challenging to

infer species-specific pathogen resistance from our results. Further studies enable us to overcome part of these problems and provide new knowledges. For example, we may use other fungus species to test the generality. We can also change resource availability in agar plug. Furthermore, we may examine the infection rate under various conditions to assess its environmental dependence. Use of mutants enables to assess the role of the gene for infection and resistance.

Conclusion

Our study revealed a strong relationship between the LES and pathogen resistance. Species employing a resource-conservative strategy exhibit greater resistance against generalist fungal pathogens like *S. sclerotiorum* that infect through the epidermis, which may contribute to their longer leaf lifespan as well as resource conservation. However, such species require an investment in biomass for cell wall reinforcement, which may compromise photosynthetic efficiency. Conversely, infection through cut surfaces showed a weak correlation with the LES, suggesting that leaf toughness is not necessarily highly effective against infections through injured tissues. Variations in chemical defense may account for the observed differences in resistance. Our experimental system offers numerous advantages for quantify pathogen resistance across various species under standardized condition; thus, it can contribute to enhancing our understanding of functional evolution in leaf traits in relation to pathogen resistance.

Data availability

All data are presented in the text or the supplemental information.

Received: 2 January 2025; Accepted: 16 June 2025
Published online: 01 July 2025

References

1. Reich, P. B., Uhl, C., Walters, M. B. & Ellsworth, D. S. Leaf lifespan as a determinant of leaf structure and function among 23 Amazonian tree species. *Oecologia* **86**, 16–24 (1991).
2. Wright, I. J. et al. The worldwide leaf economics spectrum. *Nature* **428**, 821–827 (2004).
3. Reich, P. B. The world-wide 'fast–slow'plant economics spectrum: A traits manifesto. *J. Ecol.* **102**, 275–301 (2014).
4. Hikosaka, K., Onoda, Y. & Kitajima, K. Leaf economics of deciduous and evergreen plants: How do they exhibit trait optimization under resource variations and environmental constraints. *Oecologia*, **207**, 99 (2025).
5. Onoda, Y. et al. Global patterns of leaf mechanical properties. *Ecol. lett.* **14**, 301–312 (2011).
6. Hikosaka, K. Interspecific difference in the photosynthesis–nitrogen relationship: Patterns, physiological causes, and ecological importance. *J. Plant Res.* **117**, 481–494 (2004).
7. Onoda, Y. et al. Physiological and structural tradeoffs underlying the leaf economics spectrum. *New Phytol.* **214**, 1447–1463 (2017).
8. Xue, W. et al. Cell wall thickness has phylogenetically consistent effects on the photosynthetic nitrogen-use efficiency of terrestrial plants. *Plant Cell Environ.* **46**, 2323–2336 (2023).
9. Coley P. D., Bryant, J. P. & Chapin, F. S. III. Resource availability and plant antiferbivore defense. *Science* **230**, 895–899 (1985).
10. Groom, P. K. & Lamont, B. B. Which common indices of sclerophylly best reflect differences in leaf structure?. *Écoscience* **6**, 471–474 (1999).
11. Hanley, M. E., Lamont, B. B., Fairbanks, M. M. & Rafferty, C. M. Plant structural traits and their role in anti-herbivore defence. *Perspect. Plant Ecol. Evol. Syst.* **8**, 157–178 (2007).
12. Poorter, H., Niinemets, Ü., Poorter, L., Wright, I. J. & Villar, R. Causes and consequences of variation in leaf mass per area (LMA): A meta-analysis. *New phytol.* **182**, 565–588 (2009).
13. Kitajima, K. & Poorter, L. Tissue-level leaf toughness, but not lamina thickness, predicts sapling leaf lifespan and shade tolerance of tropical tree species. *New Phytol.* **186**, 708–721 (2010).
14. Cronin, J. P., Rúa, M. A. & Mitchell, C. E. Why is living fast dangerous? Disentangling the roles of resistance and tolerance of disease. *Amer. Nat.* **184**, 172–187 (2014).
15. Cappelli, S. L., Pichon, N. A., Kempel, A. & Allan, E. Sick plants in grassland communities: A growth-defense trade-off is the main driver of fungal pathogen abundance. *Ecol. lett.* **23**, 1349–1359 (2020).
16. Yan, X. et al. Nitrogen addition and warming modulate the pathogen impact on plant biomass by shifting intraspecific functional traits and reducing species richness. *J. Ecol.* **111**, 509–524 (2023).
17. Lehner, M. S. et al. Independently founded populations of *Sclerotinia sclerotiorum* from a tropical and a temperate region have similar genetic structure. *PLoS ONE* **12**, e0173915 (2017).
18. Boland, G. J. & Hall, R. Index of plant hosts of Sclerotinia sclerotiorum. *Can. J. Plant Pathol.* **16**, 93–108 (1994).
19. Hossain, M. M.. Sultana, F., Li, W., Tran, L. S. P. & Mostofa, M. G. *Sclerotinia sclerotiorum* (Lib.) de Bary: Insights into the Pathogenomic Features of a Global Pathogen. *Cells* 12, 1063 (2023).
20. Hikosaka, K. & Shigeno, A. The role of Rubisco and cell walls in the interspecific variation in photosynthetic capacity. *Oecologia* **160**, 443–451 (2009).
21. Yasumura, Y., Hikosaka, K. & Hirose, T. Nitrogen resorption and protein degradation during leaf senescence in *Chenopodium album* grown in different light and nitrogen conditions. *Funct. Plant Biol.* **34**, 409–417 (2007).
22. Kurokawa, H. et al. Plant characteristics drive ontogenetic changes in herbivory damage in a temperate forest. *J. Ecol.* **110**, 2772–2784 (2022).
23. Albert, D., Dumonceaux, T., Carisse, O., Beaulieu, C. & Filion, M. Combining desirable traits for a good biocontrol strategy against *Sclerotinia sclerotiorum*. *Microorganisms* **10**, 1189 (2022).
24. Daleo, P. et al. Grazer facilitation of fungal infection and the control of plant growth in south-western Atlantic salt marshes. *J. Ecol.* **97**, 781–787 (2009).
25. Thaler, J. S., Agrawal, A. A. & Halitschke, R. Salicylate-mediated interactions between pathogens and herbivores. *Ecology* **91**, 1075–1082 (2010).
26. Iwase, A. et al. WIND transcription factors orchestrate wound-induced callus formation, vascular reconnection and defense response in Arabidopsis. *New Phytol.* **232**, 734–752 (2021).
27. Vance, C. P., Kirk, T. K. & Sherwood, R. T. Lignification as a mechanism of disease resistance. *Ann. Rev. Phytopathol.* **18**, 259–288 (1980).
28. Brownlee, H. E., McEuen, A. R., Hedger, J. & Scott, I. M. Anti-fungal effects of cocoa tannin on the witches' broom pathogen *Crinipellis perniciosa*. *Physiol. Mol. Plant Pathol.* **36**, 39–48 (1990).

29. Onoda, Y., Hikosaka, K. & Hirose, T. Allocation of nitrogen to cell walls decreases photosynthetic nitrogen-use efficiency. *Funct. Ecol.* **18**, 419–425 (2004).
30. Takashima, T., Hikosaka, K. & Hirose, T. Photosynthesis or persistence: Nitrogen allocation in leaves of evergreen and deciduous *Quercus* species. *Plant, Cell Environ.* **27**, 1047–1054 (2004).
31. Neilson, E. H., Goodger, J. Q. D., Woodrow, I. E. & Møller, B. L. Plant chemical defense: At what cost?. *Tre. Plant Sci.* **18**, 250–258 (2013).
32. Anderson, E. J., Ali, S., Byamukama, E., Yen, Y. & Nepal, M. P. Disease resistance mechanisms in plants. *Genes* **9**, 339 (2018).

Acknowledgement
We thank Junko Aoki for technical supports, Masako Mishio for species selection, The Botanical Garden of Tohoku University for the permission of leaf sampling and Enago (www.enago.jp) for the English language review. This study was supported by KAKENHI (20H03317, 21H05313, 23H02549).

Author contributions
K.H. designed the research. K.K. developed the infection experiment system. K.O.W. conducted the experiment. H.K. performed chemical analyses. K.O.W. and K.H wrote the paper with input from the other authors. All authors approved the final submission of the paper.

Funding
Japan Society for the Promotion of Science, 20H03317, 21H05313, 23H02549.

Declarations

Competing interests
The authors declare no competing interests.

Ethics approval
Plant leaves were harvested with relevant institutional and national guidelines and legislation.

Additional information
Supplementary Information The online version contains supplementary material available at https://doi.org/10.1038/s41598-025-07473-w.

Correspondence and requests for materials should be addressed to K.H.

Reprints and permissions information is available at www.nature.com/reprints.

Publisher's note Springer Nature remains neutral with regard to jurisdictional claims in published maps and institutional affiliations.